4,5-Dichloro-2-octyl-4-isothiazolin-3-one (DCOIT) modifies synaptic transmission in hippocampal CA3 neurons of rats

Masahito Wakita[1,2], Kiyomitsu Shoudai[2], Yasuo Oyama[3], Norio Akaike[1,4,*]

[1] Research Division for Clinical Pharmacology, Medical Corporation, Jyuryokai, Kumamoto Kinoh Hospital, Kumamoto 860-8518, Japan

[2] Research Division for Life Science, Kumamoto Health Science University, Kumamoto 861-5598, Japan

[3] Laboratory of Cellular Signaling, Faculty of Biosciences and Bioindustry, Tokushima University, Tokushima 770-8513, Japan

[4] Department of Molecular Medicine, Graduate School of Pharmaceutical Sciences, Kumamoto University, Kumamoto 862−0973, Japan.

Running title: DCOIT and Neurotransmission

[*]Corresponding author:
Norio Akaike, Ph.D., Research Director
Research Division for Clinical Pharmacology, Jyuryokai, Kumamoto Kinoh Hospital, 6-8-1 Yamamuro, Kitaku, Kumamoto 860-8518, Japan
Tel.: +81−96− 345−8111
Fax: +81−96−345−8188
E-mail address: akaike.n@juryo.or.jp (N.A.)
wakitamasahito@gmail.com (M.W.)
oyama@ias.tokushima-u.ac.jp (Y.O.)

1. Introduction

In response to the banning of organotin antifoulants, such as tributyltin and triphenyltin, chemical companies have actively developed alternative biocides (Qian et al., 2013). 4,5-Dichloro-2-octyl-4-isothiazolin-3-one (DCOIT) is supposed to be an environmentally acceptable alternative to organotin antifoulants (Jacobson and Willingham, 2000). DCOIT is the active ingredient in a series of biocide formulations marketed by the Dow Chemical Company and its global affiliates (The Dow Chemical Company, 2012). DCOIT was found in sediments of port, harbor, and coastal areas in Asian countries (Harino et al., 2007; Tsunemasa and Yamazaki, 2014; Kim et al., 2015a,b; Mochida et al., 2015). The cctanol-water partition coefficient of DCOIT is reported to be 4.5 (Shade et al., 1993) or 2.85 (Willingham and Jacobson, 1996). Thus, since there is a possibility that DCOIT accumulates in organisms, this compound may have impacts on ecosystems (Guardiola et al., 2012). The toxicity of DCOIT in wild animals is not reported. However, DCOIT is found to possess adverse actions in in vivo studies (Ito et al., 2013; Chen et al., 2014a,b, 2015, 2016). DCOIT induced apoptosis of testicular germ cells in mummichog (Ito et al., 2013). In marine Medaka, DCOIT altered oxidative stress and neurotransmission, caused endocrine disruption, and induced proteomic changes in brain and liver tissues (Chen et al., 2014a,b, 2015, 2016). DCOIT significantly inhibited acetylcholinesterase activity in the brain of marine Medaka (Chen et al., 2014a). The inhibition of acetylcholinesterase produces effects reminiscent of neurotoxicity, as described for some insecticides (Veronesi et al., 1990; Russom et al., 2014). Therefore, the aim of this study is to examine whether DCOIT has adverse actions on neuronal transmission, especially in mammalian CNS. Synaptic transmission is one of main targets for pathological and toxicological studies because it is the most vulnerable step in neuronal transmission (or signaling). Parkinson's disease, schizophrenia, dementia, and depression are related to malfunction of synaptic transmission. Therefore, this study possesses toxicological and pathological (probably biological) implications. Methyl mercury (MetHg) is one of

environmental pollutants. This compound is known to cause ‘Minamata Disease’. MetHg acts on neuronal functions including synaptic transmission in various brain regions. Thus, it is important to conduct the experiment to reveal the effects of environmental pollutants on the neuronal transmission. In this study, we examined the effects of DCOIT on synaptic transmission using a ‘synaptic bouton’ preparation (Akaike et al., 2002; Akaike and Moorhouse, 2003) isolated from hippocampus of rat brain. Hippocampal neurons are a sensitive, well-established assay for synaptic transmission function. Here, we describe the actions of DCOIT on synaptic transmission mediated by GABA and glutamate in rat brain. These actions are mediated mainly via the mobilization of intracellular Ca^{2+}. The results suggest that DCOIT at its present environmentally relevant concentrations in sea sediments may be neurotoxic in wild mammals.

2. Materials and Methods

2.1. Cell preparation – ‘synaptic bouton’ preparation

The use of experimental animals was approved by the Ethics Committee of Kumamoto Kinoh Hospital. All experiments were performed in accordance with the Guiding Principles for Care and Use of Animals in the Field of Physiological Sciences of The Physiological Society of Japan.

Details of the “synaptic bouton” preparation were described previously (Akaike et al., 2002; Akaike and Moorhouse, 2003). Briefly, Wistar rats (11−23 days old, either sex) were decapitated under pentobarbital anesthesia. The brain was removed and immersed in ice-cold oxygenated incubation medium. The ionic composition of the incubation medium was 124 mM NaCl, 5 mM KCl, 1.2 mM KH_2PO_4, 24 mM $NaHCO_3$, 2.4 mM $CaCl_2$, 1.3 mM $MgSO_4$ and 10 mM glucose. The medium was saturated with 95% O_2 and 5% CO_2 in order to adjust the pH to 7.45.

Hippocampal slices (400-μm thick) were prepared using a vibrating microtome (VR

1200S; Leica, Nussloch, Germany) and then incubated in the medium at room temperature (21−24 ºC) for at least one hour before mechanical dissociation using a fire-polished glass pipette coupled to a vibration device (S1-10 cell isolator; K.T. Labs, Tokyo). The tip of the glass pipette was placed on the surface of the slice in the hippocampal CA3 region and was vibrated horizontally (0.2−2.0 mm displacement) at 50 Hz. After dissociation, the mechanically dissociated neurons were left to settle and adhere to the bottom of the dish for at least 15 minutes.

2.2. Electrophysiological measurements

All recordings were obtained from the 'synaptic bouton' preparation of CA3 pyramidal neurons using conventional whole-cell patch-clamp recordings in voltage-clamp mode. Tables 1 and 2 show the ionic compositions of the solutions used for the current recordings. Glutamatergic evoked, spontaneous, and miniature excitatory postsynaptic currents (eEPSCs, sEPSCs, mEPSCs), and glutamate receptor-mediated currents (I_{Glu}) were recorded at a holding potential (V_H) of −65 mV. GABAergic evoked, spontaneous, and miniature inhibitory postsynaptic currents (eIPSCs, sIPSCs, mIPSCs) and $GABA_A$ receptor-mediated currents (I_{GABA}) were recorded at a V_H of 0 mV. Voltage-dependent Na^+ channel currents (I_{Na}) and Ba^{2+}-permeable high-threshold Ca^{2+} channel currents (I_{Ba}) were recorded V_Hs of −70 mV and −60 mV, respectively (Multiclamp 700B; Molecular Devices, Sunnyvale, CA) (Wakita et al., 2012). All experiments were performed at room temperature (21−24 ºC).

The resistances of the recording pipettes filled with the internal solution were 3–6 MΩ. Neuronal responses were continuously monitored on a computer display and an oscilloscope (DCS-7040; Kenwood, Tokyo, Japan). All membrane currents were acquired with 20 kHz sampling rate, filtered at 3 kHz using a low-pass filter (Multifunction Filter 3611; NF Co., Tokyo, Japan) and stored on a computer using pCLAMP 10.2 (Axon Instruments, CA, USA).

(Tables 1 and 2 near here)

Experiments were performed with wide range (0.03–10 μM) of DCOIT concentration.

One may argue the possibility that DCOIT decreases cell viability. In electrophysiological studies, it is impossible to record electrical response from dead cells or the cells with comprised membranes. Thus, electrophysiological recording reveal whether recorded cell is viable.

2.3. Paired-pulse focal electrical stimulation of single boutons using glass pipettes

Focal electric stimuli can be employed to activate a single nerve terminal in order to measure eIPSCs and eEPSCs resulting from a single presynaptic nerve ending rather than a fused event from multiple boutons. This technique offers a unique evaluation of how drugs act on pre- and post-synaptic transmission mechanisms at the single synapse level. Focal electrical stimulation of a single bouton adherent to mechanically dissociated hippocampal CA3 neurons has been described previously (Akaike et al., 2002; Akaike and Moorhouse, 2003; Wakita et al., 2012). Focal activation was achieved using a bipolar stimulating pipette (theta glass) for both current delivery and the return path in a compact format. Stimulus shocks were delivered for 100 μs at intensities of 0.06–0.1 mA with inter-stimulus intervals of 40 ms for eIPSCs and 20 ms for eEPSCs (Wakita et al., 2013). The stimulating electrode was carefully moved along the surface membrane but did not directly touch the membrane of a bouton. Periodic shocks were delivered while monitoring whole-cell currents until eIPSCs or eEPSCs appeared. These synaptic events appeared in an all-or-none fashion over a limited range of positions, which indicates that effective stimulation requires the pipette to be positioned just above the bouton (Akaike et al., 2002; Akaike and Moorhouse, 2003). Membrane resistance was not changed during the application of DCOIT because the base-line of current was not changed.

2.4. Drugs and Application

DCOIT was distributed by Tokyo Chemical Industry Co., Ltd. (Tokyo, Japan). The purity of DCOIT was >99.8%. Reagents to prepare the solutions described below were obtained from Wako Pure Chemicals (Osaka, Japan). Other reagents, such as tetraethylammonium chloride (TEA-Cl), CsCl, Cs-methanesulfonate, N-2-hydroxyethylpiperazine-N′-2-ethanesulphonic acid

(HEPES), tetrodotoxin (TTX), ethyleneglycol-bis-(α-aminoethylether)-N,N,N′,N′-tetraacetic acid (EGTA), 2-((2,6-dimethylphenyl)amino)-N,N,N-triethyl-2-oxoethanaminium (QX-314), and adenosine 5′-triphosphate magnesium salt (ATP-Mg) were obtained from Sigma Chemicals (St. Louis, MO, USA). 6-Cyano-7-nitroquinoxaline-2,3-dione (CNQX) and D-(-)-2-amino-5-phosphonovaleric acid (D-AP5) were obtained from Tocris Cookson (Ellisville, MO, USA). All test solutions containing drugs were applied using a 'Y-tube system,' which allowed solution exchange around the cells within about 20 ms (Murase et al., 1990).

2.5. Data analysis

GABAergic eIPSCs and glutamatergic eEPSCs evoked by paired-pulse focal electrical stimuli were counted and analyzed in pre-set epochs before, during, and after each test condition using pCLAMP 10.2 (Axon Instruments). The amplitudes, failure rates (Rfs), and paired-pulse ratios (PPRs) of eIPSCs and eEPSCs were analyzed using pCLAMP 10.2. PPRs were calculated by dividing the mean peak amplitude of P_2 by the mean peak amplitude of P_1. The effects of DCOIT on the current amplitudes, Rfs, and PPRs for eIPSCs and eEPSCs were normalized as relative changes with respect to their respective controls. Mean amplitude was calculated from all current responses including current amplitude = 0 (full failure).

To examine the effects of DCOIT on ionotropic inward currents induced by bath perfusions of GABA (I_{GABA}) and glutamate (I_{Glu}), 3 μM GABA and 10 μM glutamate were applied. These drug concentrations elicited little desensitization. The concentration-dependent effects of DCOIT were quantified by normalizing the peak current amplitudes in the presence of DCOIT to those in the absence of DCOIT. The relative I_{Na} and I_{Ba} responses with various concentrations of DCOIT were similarly normalized to the control peak currents in the standard solution without DCOIT.

In each experiment, sIPSCs, sEPSCs, mIPSCs, and mEPSCs were counted and analyzed in pre-set epochs before, during, and after each test condition using the MiniAnalysis Program (Synaptosoft, NJ, USA). Briefly, synaptic events were initially screened automatically using an

amplitude threshold of 10 pA and then visually accepted or rejected based upon their 10–90% rise and 90–37% decay times. The frequency, amplitude, and decay times (90−37%) of synaptic events during the control period (3 minutes) were averaged, and the frequencies, amplitudes, and decay times of all events during drug application were normalized to these control values.

All Data were analyzed using Origin Pro 7.5 software (OriginLab Corporation, Northampton, MA, USA). Data are reported as means ± S.E.M. of normalized values. Data were tested using one-way ANOVA followed by a post hoc Bonferroni test for multiple comparisons, using absolute values rather than normalized ones. Two-tailed P values of less than 0.05 were considered statistically significant.

3. Results

3.1. Effects of DCOIT on postsynaptic currents evoked by focal electrical stimulation

Synaptic boutons projecting to single CA3 neurons were stimulated by focal electrical stimulation (Akaike and Moorhouse, 2003; Akaike et al., 2002). The upper insets in Figs. 1A and 1B show typical outwardly-directed, fast eIPSCs in response to paired-pulse stimulation (40-ms interval) with and without 0.3 μM DCOIT and 10 μM DCOIT, respectively. DCOIT at 0.3 μM increased the amplitude of the current elicited by the P_1 pulse (P_1 Amp), while DCOIT at 10 μM greatly diminished the P_1 Amp. There was no recovery from the response to DCOIT after the removal of DCOIT surrounding the preparation (Figs. 1A and B).

The upper insets in Figs. 1C and 1D show typical inwardly-directed, fast eEPSCs in response to paired-pulse stimulation (20-ms interval) with and without 0.3 μM DCOIT or 10 μM DCOIT, respectively. DCOIT at 0.3 μM increased the P_1 Amp. There was recovery from the response to DCOIT after washing out. DCOIT at 10 μM significantly decreased the P_1 Amp. In this case, there was no recovery from the response to DCOIT after its removal (Figs. 1C and 1D).

(Figure 1 near here)

The concentration-dependent changes in the P_1 Amps of eIPSCs and eEPSCs elicited by DCOIT are summarized in Fig. 2A. Concentrations of DCOIT ranging from 0.03 μM to 1 μM increased the P_1 Amp, while there were decreases in response to 3–10 μM DCOIT. DCOIT at 0.03 μM decreased the value of the P_1 Rf in eEPSCs, but not eIPSCs. The Rf values of both evoked currents were reduced by 0.1–0.3 μM DCOIT, while 3−10 μM DCOIT increased these values (Fig. 2B). Similar tendencies were observed for DCOIT-induced changes in relative PPR (Fig. 2C). Thus, DCOIT biphasically modulates synaptic transmissions.

(Figure 2 near here)

3.2. Effect of DCOIT on I_{GABA} and I_{Glu} elicited by exogenous applications of GABA and glutamate

There is a possibility that DCOIT directly affects the synaptic currents evoked by focal electrical stimulation, resulting in the changes in the P_1 Amp. However, this possibility is unlikely, as DCOIT at concentrations of 0.03–3 μM did not change the amplitudes of I_{GABA} and I_{Glu} elicited by exogenous applications of GABA and glutamate (supplemental Fig. 1). Our results thus suggest that the effects of DCOIT on eIPSCs and eEPSCs resulted from its actions at presynaptic sites.

3.3. Effects of DCOIT on sIPSCs and sEPSCs

As shown in Figs. 3A and 3B, DCOIT at 10 μM significantly increases the numbers of both sIPSC and sEPSC events recorded during a period of 20 seconds. The increased numbers of events gradually decreased after the removal of DCOIT. The effects of DCOIT at 0.03–10 μM on sIPSCs and sEPSCs are summarized in Fig. 3C. DCOIT at concentrations of 1 μM or higher (up to 10 μM) significantly increases the frequency of sIPSCs in a concentration-dependent manner (Fig. 3C). Similarly, the frequency of sEPSCs was significantly increased in response to DCOIT concentrations of 0.3–10 μM. The amplitudes of sIPSCs were significantly increased by 3–10 μM DCOIT. The amplitudes of sEPSCs were only increased by 10 μM

DCOIT. The decay times of sIPSCs and eEPSCs were not affected by DCOIT at concentrations of up to 10 μM. Thus, it seems that DCOIT acts at presynaptic sites.

(Figure 3 near here)

3.4. Effects of DCOIT on mIPSCs and mEPSCs

TTX was applied under external Ca^{2+}-free conditions and mIPSCs and mEPSCs were recorded (Figs. 4A and 4B). In the presence of TTX under external Ca^{2+}-free conditions, the frequency of events was reduced. The application of 10 μM DCOIT time-dependently and markedly increased the frequencies of both mIPSCs and mEPSCs. The increases in these frequencies in response to DCOIT were statistically significant (Fig. 4C). The amplitudes of mIPSCs were reduced in the presence of TTX under external Ca^{2+}-free conditions. This reduction was statistically significant. Successive applications of 10 μM DCOIT also increased the amplitude by a small amount (Fig. 4C). A similar tendency was observed for mEPSCs. However, the changes in these amplitudes were not statistically significant.

(Figure 4 near here)

3.5. Effects of repetitive DCOIT applications on mEPSCs

As shown in Figs. 2 and 3, the frequency of EPSCs was more sensitive to DCOIT than that of IPSCs. Further studies were conducted on mEPSCs. Voltage-dependent Na^{+} and Ca^{2+} channels are not involved in responses to TTX under external Ca^{2+}-free conditions. Therefore, it is hypothesized that intracellular Ca^{2+} released from Ca^{2+} stores contributes to the increase in mEPSC frequency. DCOIT at 10 μM was repetitively applied in the presence of TTX under external Ca^{2+}-free condition. When 10 μM DCOIT was intermittently applied, the increase in mEPSC frequency decreased in a step-wise manner by the second and third applications of 10 μM DCOIT (Figs. 5A and 5Ba). However, the amplitude was not affected at all (Fig. 5Bb).

(Figure 5 near here)

3.6. Effects of DCOIT on voltage-dependent Na^+ and Ca^{2+} channel currents

Fig. 6A shows the I_{Na} recording traces without and with DCOIT. DCOIT at 3–10 μM slowed the decay phase of the I_{Na} without inducing an apparent change in current amplitude. DCOIT at concentrations ranging from 0.1 μM to 10 μM increased the decay time in a concentration-dependent manner. While the amplitude of the I_{Na} was hardly affected by DCOIT, increases in decay time of the I_{Na} due to DCOIT were statistically significant in the concentration range of 1–10 μM (Fig. 6B). On the other hand, DCOIT at 0.03−10 μM had no effects on I_{Ba} (supplemental Fig. 2).

(Figure 6 near here)

4. Discussion

4.1. DCOIT-induced changes in synaptic transmission

From the results of Figs. 1–3, DCOIT is considered to act on presynaptic nerve terminals, resulting in the facilitation of both spontaneous and action potential-dependent transmitter release. DCOIT-induced facilitation of transmitter release does not depend on Ca^{2+} influx across the plasma membrane (Fig. 4). The facilitation of transmitter release in the presence of DCOIT results from Ca^{2+} release from intracellular Ca^{2+} storage sites (Fig. 5). The present results are similar to those reported in the studies on other pollutants, such as MetHg (Juang and Yonemura, 1975), tri-n-butyltin (Kishimoto et al., 2001), and triphenyltin (Oyama et al., 1992; Wakita et al., 2015). Therefore, it may be likely that the neurotoxic actions of DCOIT are partly similar to those of organometals.

The increase in the frequency of mEPSCs was counteracted by repetitive applications of DCOIT in the Ca^{2+}-free solution containing TTX (Fig. 5). Thus, the repetitive DCOIT applications deplete the Ca^{2+} in intracellular Ca^{2+} stores in nerve endings. Such Ca^{2+} depletion may also be involved in the inhibition of action potential-dependent transmitter release at high DCOIT concentration because of following reasons. The Ca^{2+}-induced Ca^{2+} release (CICR)

(Verkhratsky and Shmigol, 1996) is activated by Ca^{2+} influx through voltage-dependent Ca^{2+} channels that were not inhibited by DCOIT. Therefore, there is another possibility that DCOIT inhibit CICR via a Ca^{2+} depletion of calcium stores, resulting in the depression of action potential-dependent transmitter release. One may argue a following possibility. The distribution of voltage-dependent Ca^{2+} channel subtypes in postsynaptic membranes might be different from that in presynaptic membranes. However, our previous studies showed that the difference of Ca^{2+} channel subtypes between pre- and postsynaptic membrane are a little. On this matter, we investigated electrophysiologically what kinds of Ca^{2+} channel subtypes exist in presynaptic nerve terminals (Murakami et al., 2002; Shin et al., unpublished observation).

In previous studies (Yamamoto et al., 2011, Wakita et al., 2012), the large depolarization of presynaptic nerve terminals facilitates spontaneous transmitter release, but inhibits action potential-dependent release by blockage of Na^{+} channels. At high concentration DCOIT induced a slight increase in I_{Na} decay time (Fig. 6), possibly resulting in prolonged action potential. Therefore, one may argue a possibility that the prolongation of action potential by DCOIT sustainably depolarizes the presynaptic terminals, resulting in the depression of action potential-dependent transmitter release. However, it seems to be unlikely because the slight prolongation of action potential by DCOIT is not enough to consistently depolarize the presynaptic membranes.

The effects of DCOIT were about 10 to 30 times greater on eIPSCs and eEPSCs than on spontaneous currents. In addition, the former was drained much faster than the latter. It is well-known that the release of both GABA and glutamate at many synapses is facilitated by a presynaptic cAMP increase, which activates PKA and the phosphorylation of presynaptic proteins involved in vesicle cycling and/or exocytosis (Chavis et al., 1998; Turner et al., 1999). Other reports show the cAMP modulates release via PKA-independent mechanisms (Sakaba and Neher, 2001; Kaneko and Takahashi, 2004). According to Katsurabayashi et al. (2004), glycinergic eIPSCs are regulated via a PKA-dependent pathway, while sIPSCs are modulated directly by cAMP and/or PKA-independent pathways. Therefore, previous reports suggest that

DCOIT may differentially modulate intracellular release mechanisms in evoked vs. spontaneous synaptic transmission.

4.2. Some technical aspects

Usually, action-potential evoked eIPSCs recorded at a single synapse level show large variance from 0 to about 200 pA in current amplitudes as shown in a case of Fig. 1A. Here, we have to remind that a single neuronal cell body receives many excitatory or inhibitory synaptic inputs from a few hundred to thousand. Therefore, eIPSC and eEPSC of previous reports recorded in brain slice preparation are the averaged current amplitude of many input currents. Consequently, these synaptic currents of slice preparation show almost steady current amplitude. Please note that there is large difference between the current amplitude variance between currents recorded from single synapses in our synapse-bouton preparation and from multi synapses in conventional slice preparation.

Since we calculated the average current amplitude of all currents including full failure, we can compare statistically the current difference between control and the presence of DCOIT.

The concentration response curves for either eEPSC or eIPSC are not unusual. Because, DCOIT facilitates transmitter release at low concentration but inhibits the release at high concentration. DCOIT at high concentration induces the depletion of transmitter by acting transmitter release machinery in nerve endings, as seen in Fig. 5A. Similar observations were reported in our previous report (Wakita et al., 2015) and Juang and Yonemura (1975) using MetHg.

4.3. Toxicological implications

DCOIT is an alternative antifouling biocide that may have a significant impact on ecosystems (Guardiola et al., 2012). Toxic actions of DCOIT and other isothiazolone biocides have previously been reported (Williams, 2007; Thomas and Brooks, 2010). However, apparent neurotoxic actions of DCOIT have not been reported until now. We observed that DCOIT

significantly facilitates synaptic transmission mediated by GABA and glutamate in rat hippocampal CA3 neurons (Figs. 3–5). In addition, DCOIT may potentiate the transmission mediated by acetylcholine, as it inhibits acetylcholinesterase activity (Chen et al., 2014a). Thus, DCOIT is thought to affect both inhibitory and excitatory transmission. DCOIT is found in harbors, bays, and coastal areas worldwide (Steen et al., 2004; Harino et al., 2012; Lee et al., 2015; Mochida et al., 2015). The concentration of DCOIT in marine sediment varies from 'not detected' to several hundred μg/kg. Therefore, it may not be surprising to find local high concentrations of DCOIT everywhere. In the product safety assessment released from the Dow Chemical Company (2012), DCOIT is suggested to have a low risk of accumulating in the food chain. It is difficult to suggest the in vivo neurotoxicity based on our in vitro results, as the in vitro concentrations of DCOIT that had significant effects on synaptic transmission were 1–10 μM (equivalent values; 282–2,822 μg/L). Thus, the changes in fundamental transmission may represent the potential for neurotoxic effects. In a study by Chen et al. (2014b), the marine medaka (Oryzias melastigma) was exposed to DCOIT at 9 nM (2.55 μg/L) for 28 days in order to examine proteomic changes in brain tissue. eEPSCs and eIPSCs were immediately affected by 0.03 μM and 0.1 μM (equivalent values; 8.4 μg and 28.1 μg) DCOIT, respectively (Fig. 2). Long-term exposure to lower concentrations of DCOIT may change neurotransmission and result in neurotoxicity. The concentrations of DCOIT ranged from 0.04 μg/kg to 281 μg/kg dry sediment collected from Ostuki Bay, Japan (Hirano et al., 2007), Hiroshima Bay, Japan (Tsunemasa and Yamazaki, 2014; Mochida et al., 2015), and Busan Bay and Coast, South Korea (Kim et al., 2015a,b). The octanol-water partition coefficient of DCOIT is reported to be 4.5 (Shade et al., 1993) or 2.85 (Willingham and Jacobson, 1996). Thus, there is a possibility that DCOIT accumulates in organisms.

Acknowledgements

This work was supported by Grants-in-Aid from Kumamoto Health Science University for K. Shoudai and M. Wakita (2015-C-04) and from Kumamoto Kinoh Hospital for N. Akaike and M. Wakita.

Conflict of interest statement

We have no conflicts of interests to declare.

References

Akaike, N., Moorhouse, A.J., 2003. Techniques: applications of the nerve-bouton preparation in neuropharmacology. Trends Pharmacol. Sci. 24, 44−47.

Akaike, N., Murakami, N., Katsurabayashi, S., Jin, Y.H., Imazawa, T., 2002. Focal stimulation of single GABAergic presynaptic boutons on the rat hippocampal neuron. Neurosci. Res. 42, 187−195.

Chavis, P., Mollard, P., Bockaert, J., Manzoni, O., 1998. Visualization of cyclic AMP-regulated presynaptic activity at cerebellar granule cells. Neuron 20, 773−781.

Chen, L., Sun, J., Zhang, H., Au, D.W., Lam, P.K., Zhang, W., Bajic, V.B, Qiu, J.W., & Qian, P.Y., 2015. Hepatic proteomic responses in marine medaka (Oryzias melastigma) chronically exposed to antifouling compound butenolide [5-octylfuran-2 (5H)-one] or 4, 5-dichloro-2-n-octyl-4-isothiazolin-3-one (DCOIT). Environ. Sci. Technol. 49, 1851−1859.

Chen, L., Ye, R., Xu, Y., Gao, Z., Au, D.W., Qian, P.Y., 2014a. Comparative safety of the antifouling compound butenolide and 4,5-dichloro-2-n-octyl-4-isothiazolin-3-one (DCOIT) to the marine medaka (Oryzias melastigma). Aquat. Toxicol. 149, 116–125.

Chen, L., Zhang, H., Sun, J., Wong, Y.H., Han, Z., Au, D.W., Bajic, V.B., Qian, P.Y., 2014b. Proteomic changes in brain tissues of marine medaka (Oryzias melastigma) after chronic exposure to two antifouling compounds: Butenolide and 4, 5-dichloro-2-n-octyl-4-isothiazolin-3-one (DCOIT). Aquat. Toxicol, 157, 47–56.

Chen, L., Zhang, W., Ye, R., Hu, C., Wang, Q., Seemann, F., Au, D.W., Zhou, B., Giesy, J.P., Qian, P.Y., 2016. Chronic exposure of marine medaka (Oryzias melastigma) to 4, 5-dichloro-2-n-octyl-4-isothiazolin-3-one (DCOIT) reveals its mechanism of action in endocrine disruption via the hypothalamus-pituitary-gonadal-liver (HPGL) axis. Environ. Sci. Technol. 50, 4492−4501.

Guardiola, F.A., Cuesta, A., Meseguer, J., Esteban, M.A., 2012. Risks of using antifouling biocides in aquaculture. Int. J. Mol. Sci. 13, 1541−1560.

Harino, H., Arifin, Z., Rumengan, I.F., Arai, T., Ohji, M., Miyazaki, N., 2012. Distribution of

antifouling biocides and perfluoroalkyl compounds in sediments from selected locations in Indonesian coastal waters. Arch. Environ. Contam. Toxicol. 63, 13–21.

Harino, H., Yamamoto, Y., Eguchi, S., Kurokawa, Y., Arai, T., Ohji, M., Okamura H, Miyazaki, N., 2007. Concentrations of antifouling biocides in sediment and mussel samples collected from Otsuchi Bay, Japan. Arch. Environ. Contam. Toxico. 52, 179.

Ito, M., Mochida, K., Ito, K., Onduka, T., Fujii, K., 2013. Induction of apoptosis in testis of the marine teleost mummichog Fundulus heteroclitus after in vivo exposure to the antifouling biocide 4, 5-dichloro-2-n-octyl-3 (2H)-isothiazolone (Sea-Nine 211). Chemosphere 90, 1053−1060.

Jacobson, A.H., Willingham, G.L., 2000. Sea-nine antifoulant: an environmentally acceptable alternative to organotin antifoulants. Sci. Total Environ. 258, 103–110.

Juang, M.S., Yonemura, K., 1975. Increased spontaneous transmitter release from presynaptic nerve terminal by methylmercuric chloride. Nature 256, 211−213.

Kaneko, M., Takahashi, T., 2004. Presynaptic mechanism underlying cAMP-dependent synaptic potentiation. J. Neurosci. 24, 5202−5208.

Katsurabayashi, S., Kubota, H., Moorhouse, A.J., Akaike, N., 2004. Differential modulation of evoked and spontaneous glycine release from rat spinal cord glycinergic terminals by the cyclic AMP/protein kinase A transduction cascade. J Neurochem. 91, 657−666.

Kim, N.S., Hong, S.H., An, J.G., Shin, K.H., Shim, W.J., 2015a. Distribution of butyltins and alternative antifouling biocides in sediments from shipping and shipbuilding areas in South Korea. Marine Pollu. Bull. 95, 484−490.

Kim, U.J., Lee, I.S., Choi, M.,Oh, J.E., 2015b. Assessment of organotin and tin-free antifouling paints contamination in the Korean coastal area. Marine Pollu. Bull. 99, 157−165.

Kishimoto, K., Matsuo, S.I., Kanemoto, Y., Ishibashi, H., Oyama, Y., Akaike, N., 2001. Nanomolar concentrations of tri-n-butyltin facilitate gamma-aminobutyric acidergic synaptic transmission in rat hypothalamic neurons. J. Pharmacol. Exp. Ther. 299, 171–177.

Lee, M.R., Kim, U.J., Lee, I.S., Choi, M., Oh, J.E., 2015. Assessment of organotin and tin-free

antifouling paints contamination in the Korean coastal area. Mar. Pollut. Bull. 99, 157–165.

Mochida, K., Hano, T., Onduka, T., Ichihashi, H., Amano, H., Ito, M., Ito, K., Tanaka, H., Fujii, K., 2015. Spatial analysis of 4, 5-dichloro-2-n-octyl-4-isothiazolin-3-one (Sea-Nine 211) concentrations and probabilistic risk to marine organisms in Hiroshima Bay, Japan. Environ. Pollut. 204, 233–240.

Murase, K., Randic, M., Shirasaki, T., Nakagawa, T., Akaike, N., 1990. Serotonin suppresses N-methyl-D-aspartate responses in acutely isolated spinal dorsal horn neurons of the rat. Brain Res. 525, 84–91.

Oyama, Y., Chikahisa, L., Hayashi, A., Ueha, T., Sato, M., Matoba, H., 1992. Triphenyltin-induced increase in the intracellular Ca^{2+} of dissociated mammalian CNS neuron: its independence from voltage-dependent Ca^{2+} channels. Jpn. J. Pharmacol. 58, 467–471.

Qian, P.Y., Chen, L., Xu, Y., 2013. Mini-review: Molecular mechanisms of antifouling compounds. Biofouling. 29, 381–400.

Russom, C.L., LaLone, C.A., Villeneuve, D.L., Ankley, G.T., 2014. Development of an adverse outcome pathway for acetylcholinesterase inhibition leading to acute mortality. Environ. Toxicol. Chem. 33, 2157–2169.

Sakaba, T., Neher, E., 2001. Preferential potentiation of fast-releasing synaptic vesicles by cAMP at the calyx of Held. Proc. Natl. Acad. Sci. U. S. A. 98, 331−336.

Shade, W.D., Hurt, S.S., Jacobson, A.H., Reinert, K.H., 1993. Ecological risk assessment of a novel marine antifoulant. In: Gorsuch, J.W., Dwyer, F.J., Ingersoll, C.G., La Point, T.W. (Eds.), Environmental Toxicology and Risk Assessment, ASTM STP 1173, vol. 2. American Society for Testing and Materials, Philadelphia, USA, pp. 381–408.

Steen, R.J., Ariese, F., van Hattum, B., Jacobsen, J., Jacobson, A., 2004. Monitoring and evaluation of the environmental dissipation of the marine antifoulant 4, 5-dichloro-2-n-octyl-4-isothiazolin-3-one (DCOIT) in a Danish Harbor. Chemosphere 57, 513–521.

The Dow Chemical Company, 2012. Product Safety Assessment.4,5-Dichloro-2-octyl-4-isothiazolin-3-one (DCOIT).

http://www.dow.com/webapps/lit/litorder.asp?filepath=productsafety/pdfs/noreg/233-00821.pdf&pdf=true.

The Standing Committee on Biocidal Products of EC, 2014. Assessment Report. 4,5-Dichloro-2-octyl-2H-isothiazol-3-one (DCOIT) https://circabc.europa.eu/sd/a/5d2b12c8-7690-4636-a962-ab277f4b183d/DCOIT

Thomas, K.V., Brooks, S., 2010. The environmental fate and effects of antifouling paint biocides. Biofouling. 26, 73–88.

Tsunemasa, N., Yamazaki, H., 2014. Concentration of antifouling biocides and metals in sediment core samples in the northern part of Hiroshima Bay. Int. J. Molec. Sci. 15, 9991−10004.

Turner, K.M., Burgoyne, R.D., Morgan, A., 1999. Protein phosphorylation and the regulation of synaptic membrane traffic. Trends Neurosci. 22, 459−464.

Verkhratsky, A., Shmigol, A., 1996. Calcium-induced calcium release in neurones. Cell Calcium. 19, 1–14.

Veronesi, B., Jones, K., Pope, C., 1990. The neurotoxicity of subchronic acetylcholinesterase (AChE) inhibition in rat hippocampus. Toxicol. Appl. Pharmacol. 104, 440–456.

Wakita, M., Kotani, M., Nonaka, K., Shin, M.C., Akaike, N., 2013. Effects of propofol on GABAergic and glutamatergic transmission in isolated nerve-synapse preparations. Eur. J. Pharmacol. 718, 63−73.

Wakita, M., Oyama, Y., Takase, Y., Akaike, N., 2015. Modulation of excitatory synaptic transmission in rat hippocampal CA3 neurons by triphenyltin, an environmental pollutant. Chemosphere 120, 598−607.

Wakita, M., Shin, M.C., Iwata, S., Nonaka, K., Akaike, N., 2012. Effects of ethanol on $GABA_A$ receptors in GABAergic and glutamatergic presynaptic nerve terminals. J. Pharmacol. Exp. Ther. 341, 809−819.

Willingham, G. L., & Jacobson, A. H. (1996). Designing an environmentally safe marine antifoulant. ACS Symp 640. Designing Safer Chmeicals, Green Chemistry for Prevention, pp. 244-233.

Williams, T.M., 2007. The mechanism of action of isothiazolone biocides. Power Plant Chem. 9, 14–22.

Yamamoto, S., Yoshimura, M., Shin, M.C., Wakita, M., Nonaka, K., Akaike, N., 2011. GABA(A) receptor-mediated presynaptic inhibition on glutamatergic transmission. Brain Res. Bull. 84, 22−30.

Figure Captions

Figure 1. Effects of 0.3 and 10 μM DCOIT on GABAergic eIPSCs (A, B) and glutamatergic eEPSCs (C, D) evoked by paired-pulse focal electrical stimuli. Representative eIPSCs evaluated by paired-pulse stimulation before (1), during (2), and after (3) adding 0.3 (Aa) and 10 μM DCOIT (Ba). Current traces *1*, *2*, and *3* were obtained at time points *1*, *2*, and *3* in (Ab) and (Bb), respectively. Each arrowhead indicates the peak of the P_1 (filled arrowhead) and P_2 (open arrowhead) eIPSC current amplitudes. Plots of the P_1 current amplitudes of eIPSCs against time in the absence (open circle) and presence (gray circle) of 0.3 (Ab) and 10 μM DCOIT (Bb). Electrical stimuli that failed to evoke eIPSCs (i.e., amplitude = 0) were counted as failures and used to calculate the failure rate (Rf) of eIPSCs. Typical eEPSCs before (1), during (2), and after (3) the application of 0.3 (Ca) and 10 μM DCOIT (Da). Typical time courses of the P_1 amplitude of eEPSCs before, during, and after the application of 0.3 (Cb) and 10 μM DCOIT (Db).

Figure 2. Mean relative P_1 current amplitude (A), P_1 Rf (B), and PPR (C) of eIPSCs (gray bars) and eEPSCs (solid bars) evaluated by paired-pulse focal stimulation during the application of DCOIT at various concentrations (0.03–10 μM),. Each bar represents mean ± standard error of the mean (SEM). Data were obtained from 5–9 neurons.* $P < 0.05$, ** $P < 0.01$, *** $P < 0.001$.

Figure 3. Effects of DCOIT on GABAergic sIPSCs and glutamatergic sEPSCs. Typical time courses of sIPSC (Aa) and sEPSC (Ba) frequencies before, during, and after adding 10 μM DCOIT, indicated by the black bar. Typical current traces - *1* (control), *2* (10 μM DCOIT), and *3* (washout) - of sIPSCs (Ab) and sEPSCs (Bb), obtained from the corresponding time points of *1*, *2*, and *3* in (Aa) and (Ba), respectively. (C) Mean relative frequencies (Freq., a), amplitudes (Amp., b), and decay times (c) of sIPSCs (gray bars) and sEPSCs (solid bars) during the application of DCOIT at various concentrations (0.03–10 μM). All parameters were normalized to values obtained in the absence of DCOIT. Each bar represents the mean ± SEM of data obtained from 4 to 9 neurons. * $P < 0.05$, ** $P < 0.01$.

Figure 4. Effects of DCOIT on GABAergic mIPSCs and glutamatergic mEPSCs. Typical time courses of

mIPSC (Aa) and mEPSC (Ba) frequencies in control conditions before, during, and after the application of 10 μM DCOIT (black bar) in the presence of 300 nM TTX in a Ca^{2+}-free external solution (gray bar). Typical current traces - *1* (control), *2* (TTX + Ca^{2+}-free), and *3* (TTX + Ca^{2+}-free + 10 μM DCOIT) - of mIPSCs (Ab) and mEPSCs (Bb), obtained from the corresponding time points *1*, *2*, and *3* in (Aa) and (Ba), respectively. (C) Mean relative frequencies (Freq., a) and amplitudes (Amp., b) of mIPSCs (gray bars) and mEPSCs (solid bars) under control conditions and in the presence of 300 nM TTX + Ca^{2+}-free and 300 nM TTX + Ca^{2+}-free + 10 μM DCOIT, respectively. Each bar represents the mean ± SEM of data obtained from 5 neurons. * $P < 0.05$, ** $P < 0.01$.

Figure 5. Effects of repetitive (3 times) DCOIT application on glutamatergic mEPSCs. A typical time course of mEPSC frequency in control conditions and before, during, and after the repetitive (3 times) application of 10 μM DCOIT (black bar) in the presence of 300 nM TTX in a Ca^{2+}-free external solution (gray bar). (B) Mean relative frequencies (Freq., a) and amplitudes (Amp., b) of mEPSCs under control conditions and in the presence of 300 nM TTX + Ca^{2+}-free and 300 nM TTX + Ca^{2+}-free + 10 μM DCOIT 1, DCOIT 2, and DCOIT 3, respectively. Each bar represents the mean ± SEM of data obtained from 5 neurons. * $P < 0.05$, *** $P < 0.001$.

Figure 6. Effects of DCOIT on I_{Na}. I_{Na} was elicited by a test pulse from a V_H of –70 mV to –20 mV. Typical current traces of I_{Na} during and after the application of 3 and 10 μM DCOIT (A). The effects of various concentrations of DCOIT on the peak amplitudes (Amp) of the inward currents are expressed relative to the amplitude of the current response obtained in the absence of DCOIT (Ba). The effects of various concentrations of DCOIT on the decay times (90% to 37%) of the inward currents are expressed relative to the decay time of the current response obtained in the absence of DCOIT (Bb). Each bar represents the mean ± SEM of data obtained from 4 to 7 neurons.

Figure 1

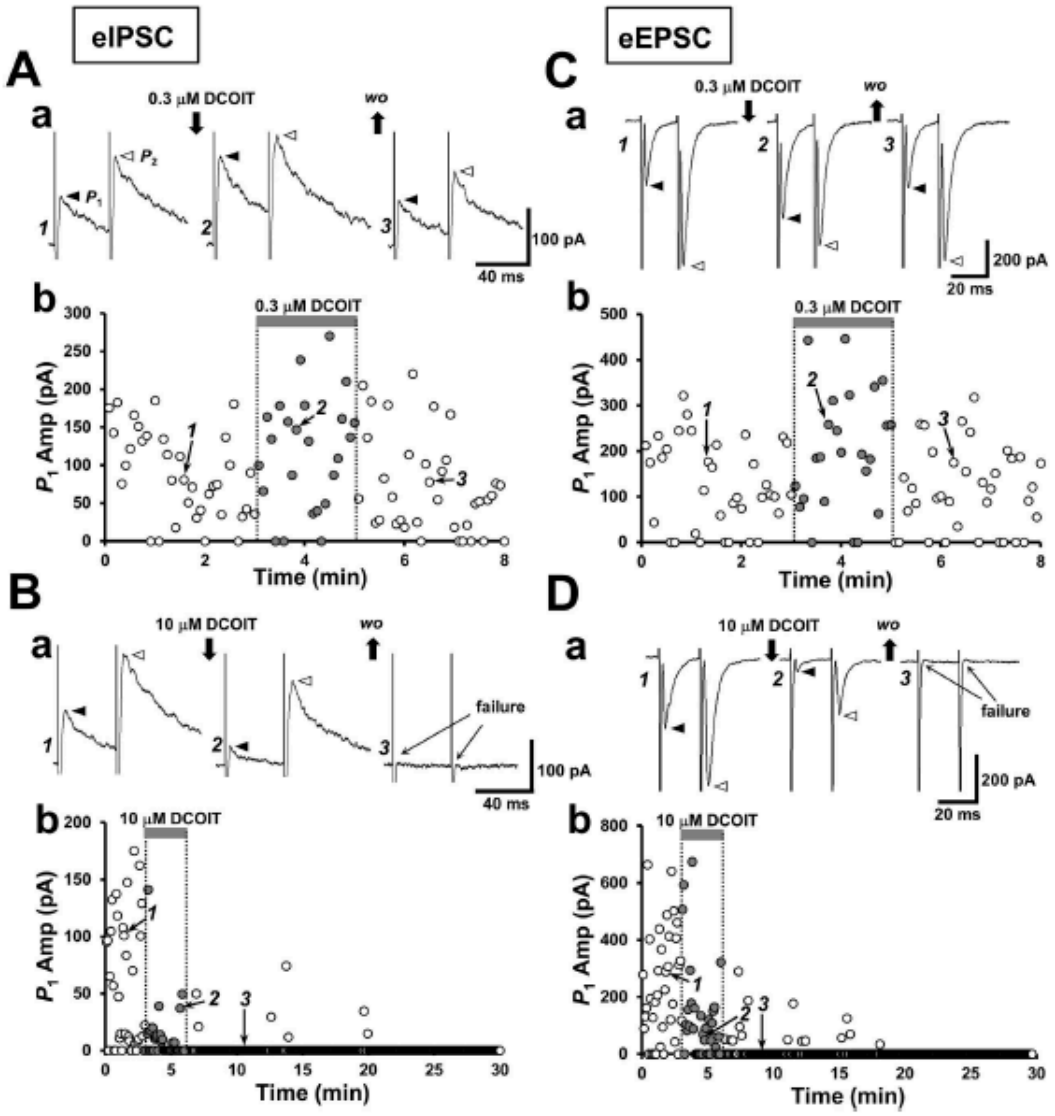
eIPSC
eEPSC
A
B
C
D
a
b
0.3 μM DCOIT
10 μM DCOIT
wo
failure
100 pA
40 ms
200 pA
20 ms
P1 Amp (pA)
Time (min)

Figure 2

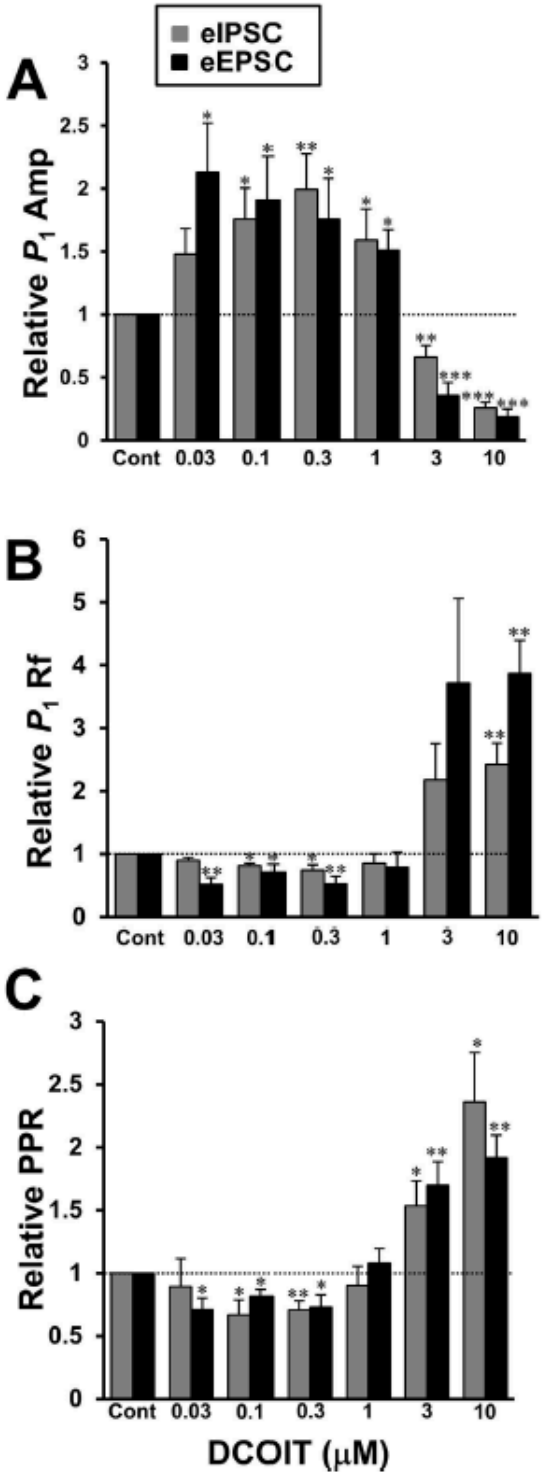
A
eIPSC
eEPSC
Relative P_1 Amp
3
2.5
2
1.5
1
0.5
0
Cont 0.03 0.1 0.3 1 3 10
B
Relative P_1 Rf
6
5
4
3
2
1
0
Cont 0.03 0.1 0.3 1 3 10
C
Relative PPR
3
2.5
2
1.5
1
0.5
0
Cont 0.03 0.1 0.3 1 3 10
DCOIT (μM)

Figure 3

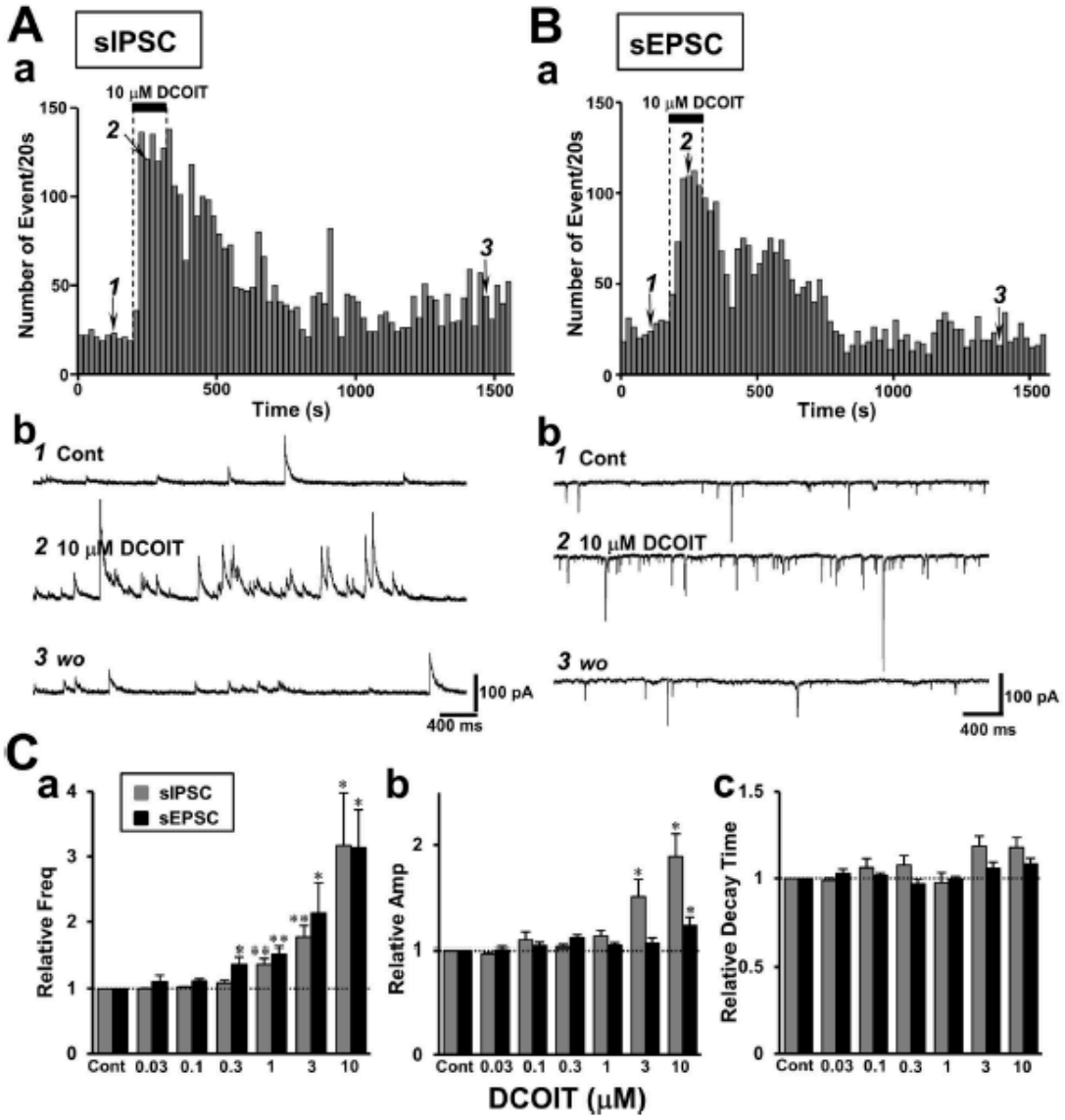
A
sIPSC
a
10 μM DCOIT
Number of Event/20s
Time (s)
b
1 Cont
2 10 μM DCOIT
3 wo
100 pA
400 ms
B
sEPSC
C
a
sIPSC
sEPSC
Relative Freq
b
Relative Amp
c
Relative Decay Time
Cont 0.03 0.1 0.3 1 3 10
DCOIT (μM)

Figure 4

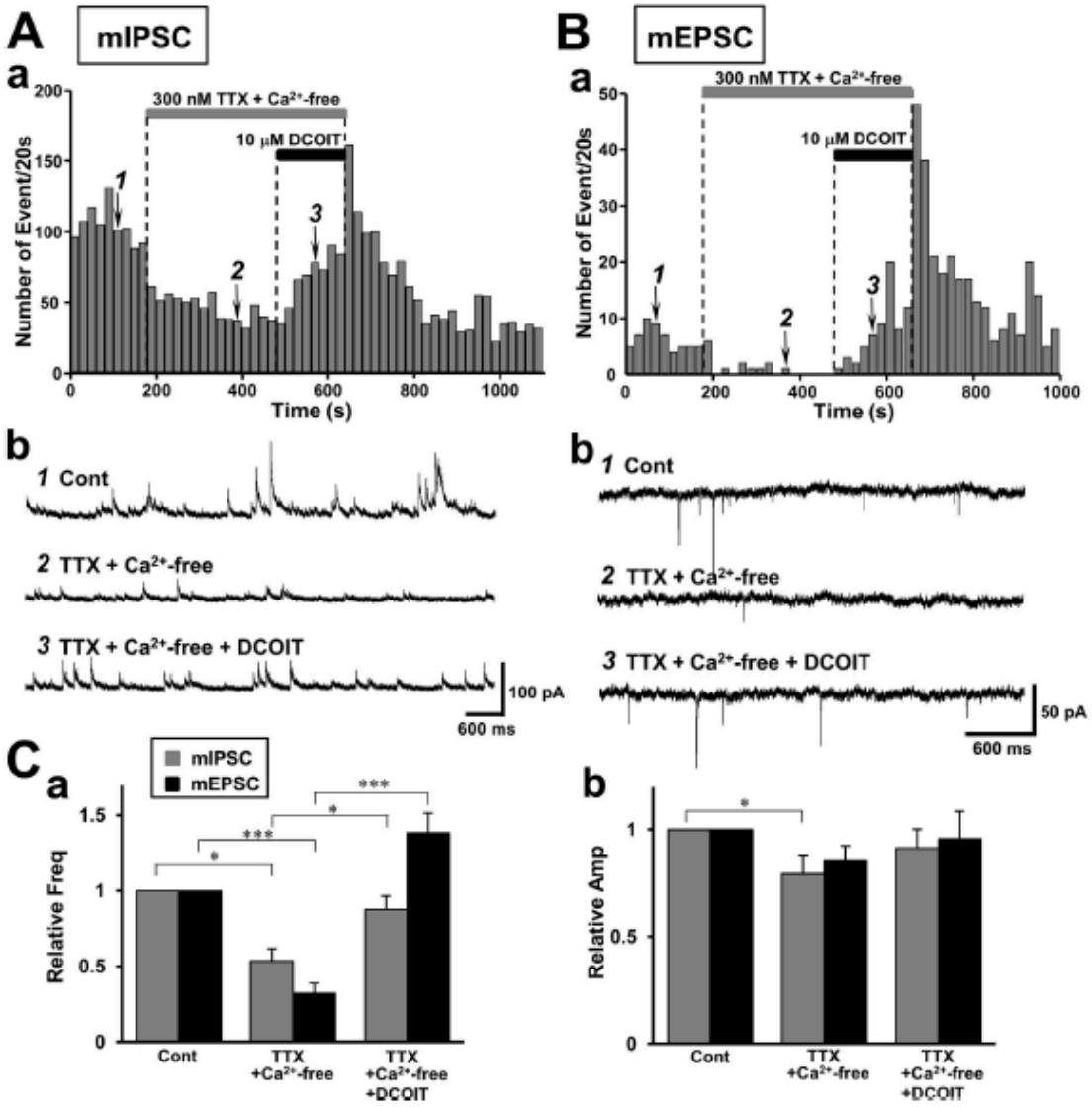
A
mIPSC
a
300 nM TTX + Ca2+-free
10 μM DCOIT
Number of Event/20s
Time (s)
b
1 Cont
2 TTX + Ca2+-free
3 TTX + Ca2+-free + DCOIT
100 pA
600 ms
B
mEPSC
a
300 nM TTX + Ca2+-free
10 μM DCOIT
Number of Event/20s
Time (s)
b
1 Cont
2 TTX + Ca2+-free
3 TTX + Ca2+-free + DCOIT
50 pA
600 ms
C
a
mIPSC
mEPSC
Relative Freq
Cont
TTX +Ca2+-free
TTX +Ca2+-free +DCOIT
b
Relative Amp
Cont
TTX +Ca2+-free
TTX +Ca2+-free +DCOIT

Figure 5

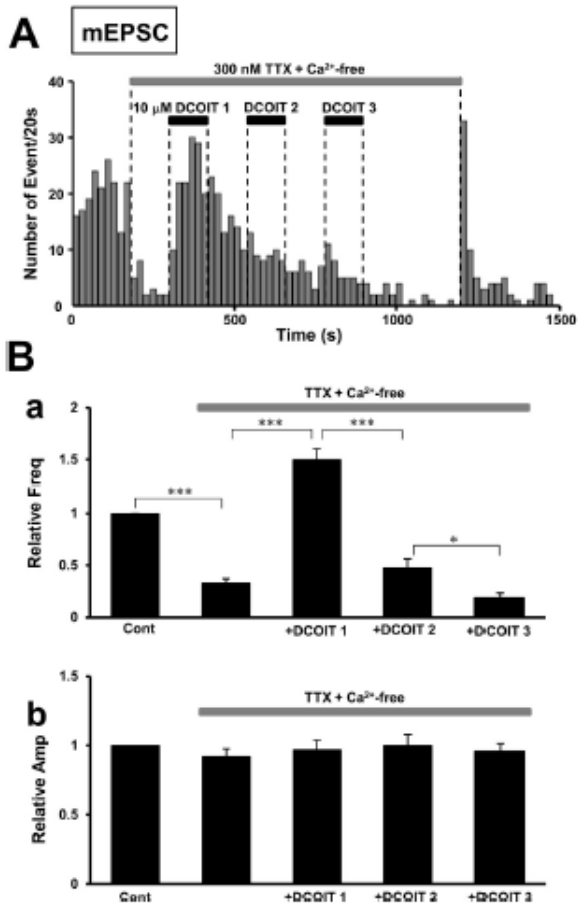
A
mEPSC
300 nM TTX + Ca2+-free
10 μM DCOIT 1
DCOIT 2
DCOIT 3
Number of Event/20s
Time (s)
B
a
TTX + Ca2+-free
Relative Freq
Cont
+DCOIT 1
+DCOIT 2
+DCOIT 3
b
TTX + Ca2+-free
Relative Amp
Cont

Figure 6

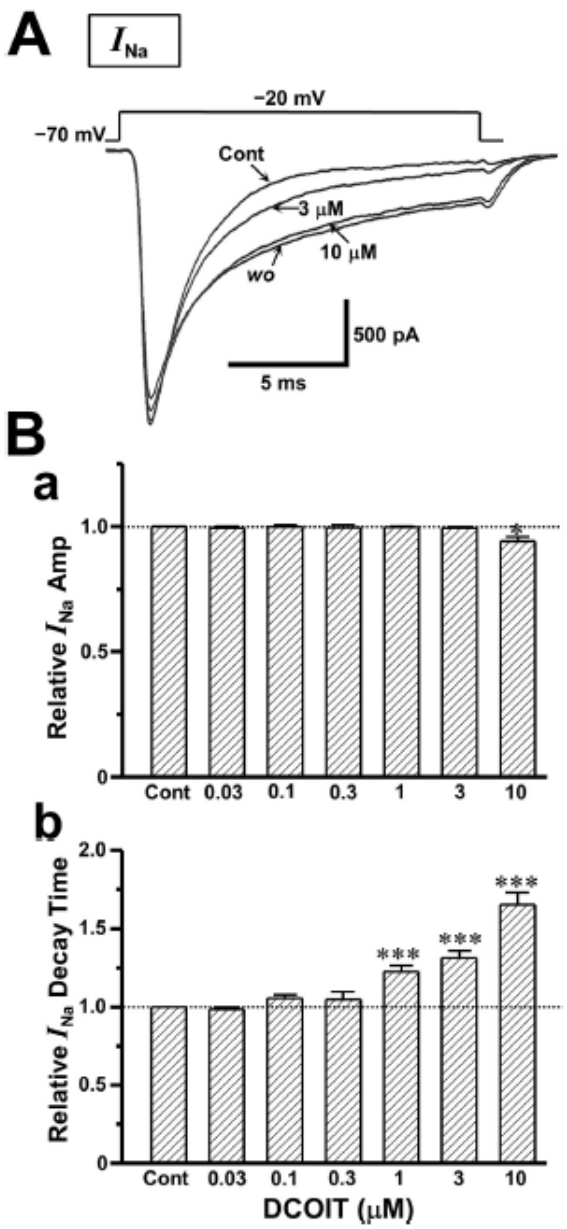
A
I_{Na}
−20 mV
−70 mV
Cont
3 μM
10 μM
wo
500 pA
5 ms
B
a
Relative I_{Na} Amp
1.0
0.5
0
Cont 0.03 0.1 0.3 1 3 10
b
Relative I_{Na} Decay Time
2.0
1.5
1.0
0.5
0
***
***
***
Cont 0.03 0.1 0.3 1 3 10
DCOIT (μM)

Table 1

Solutions for recording currents elicited by GABA and glutamate.

Recording Currents	External Solution	Internal Pipette Solution
GABAergic IPSC and I_{GABA}		
Ionic Composition	150 mM NaCl	5 mM CsCl
	5 mM KCl	135 mM Cs-methanesulfonate
	2 mM $CaCl_2$	5 mM TEA-Cl
	1 mM $MgCl_2$	10 mM EGTA
	10 mM Glucose	10 mM HEPES
	10 mM HEPES	4 mM ATP-Mg
	pH 7.4	pH 7.2
	Adjusted with Tris base	Adjusted with Tris base
Glutamatergic EPSC and I_{Glu}		
Ionic Composition	150 mM NaCl	5 mM CsCl
	5 mM KCl	135 mM CsF
	2 mM $CaCl_2$	5 mM TEA-Cl
	1 mM $MgCl_2$	2 mM EGTA
	10 mM Glucose	10 mM HEPES
	10 mM HEPES	5 mM QX-314 bromide
	pH 7.4	pH 7.2
	Adjusted with Tris base	Adjusted with Tris base

Table 2

Solutions for recording voltage-dependent currents.

Recording Current	External Solution	Internal Pipette Solution
Voltage-dependent Na^+ Current (I_{Na})		
Ionic Composition	60 mM NaCl	105 mM CsF
	100 mM Choline -Cl	30 mM NaF
	10 mM CsCl	5 mM CsCl
	10 mM glucose	5 mM TEA-Cl
	0.01 mM $LaCl_3$	2 mM EGTA
	5 mM TEA-Cl	10 mM HEPES
	10 mM HEPES	2 mM ATP-Mg
	pH 7.4	pH 7.2
	Adjusted with Tris base	Adjusted with Tris base
Ba^{2+} Current (I_{Ba}) through Voltage-dependent Ca^{2+} Channels		
Ionic Composition	145 mM Choline-Cl	80 mM Cs-methanesulfonate
	5 mM CsCl	60 mM CsCl
	5 mM $BaCl_2$	5 mM TEA-Cl
	1 mM $MgCl_2$	2 mM EGTA
	10 mM glucose	10 mM HEPES
	10 mM HEPES	2 mM ATP-Mg
	pH 7.4	pH 7.2
	Adjusted with Tris base	Adjusted with Tris base